Grain refinement effect on hydrogen embrittlement resistance of an equiatomic CoCrFeMnNi high-entropy alloy

Short communications

Grain refinement effect on hydrogen embrittlement resistance of an equiatomic CoCrFeMnNi high-entropy alloy

Motomichi Koyama*, Kenshiro Ichii, Kaneaki Tsuzaki

Department of mechanical engineering, Kyushu University, Motooka 744, Fukuoka 819-0395, Japan

*Corresponding author: Motomichi Koyama

e-mail: koyama@mech.kyushu-u.ac.jp

Abstract

We investigated the grain refinement effect on the resistance to hydrogen embrittlement in an equiatomic CoCrFeMnNi high-entropy alloy. In a 100 MPa hydrogen gas pre-charging condition, grain refinement to 1.9 μm improved the hydrogen embrittlement resistance in terms of the strength-elongation balance. In particular, the tensile strength of the grain refined high-entropy alloy did not decrease by hydrogen uptake. However, when the σ phase formed at a relatively low temperature, both the strength and elongation decreased due to hydrogen charging.

Keywords: Hydrogen embrittlement; grain refining; austenitic steels; high-entropy alloy; hydrogen desorption

1. Introduction

Increasing configurational entropy is a new alloy design strategy for improving mechanical performance [1, 2]. The compositional complexity endows a superior strength-ductility balance [3], cryogenic toughness [4], and corrosion resistance [5]. Therefore, this alloy design strategy is expected to provide drastic improvements in the mechanical performance. In particular, an equiatomic CoCrFeMnNi high-entropy alloy (HEA) with a face centered cubic (FCC) structure has gained attention as a new class of hydrogen-resistant high-strength alloys [6-9]. For example, when the HEA was exposed to 15-MPa-hydrogen gas, no significant degradation in the tensile properties was observed with a strain rate of 10^{-4} s^{-1} [6], which is comparable to stable austenitic steels that have been recognized as the highest grade of hydrogen-resistant alloys [10-12]. However, when exposed to 100-MPa-hydrogen gas [8] or tested at a strain rate of 10^{-6} s^{-1} [7], hydrogen-induced mechanical degradation was observed in the HEA. In both the cases, intergranular cracking is the key to further improvements of the hydrogen embrittlement resistance [7, 8].

For intergranular cracking, grain refinement has acted as an effective method for preventing grain boundary decohesion, owing to the reduction in hydrogen content per unit grain boundary area and a reduction in the local stress concentration at grain boundaries [13]. Similarly, hydrogen-assisted intergranular cracking in FCC metals/alloys, such as austenitic steels, is suppressed with decreasing grain size [14-16]. Therefore, grain refinement effects on the hydrogen embrittlement of HEAs have undoubtedly attracted a great deal of attention in hydrogen-related research fields.

2. Experimental procedure

In order to investigate the grain refinement effect, a 50 kg ingot of the equiatomic

CoCrFeMnNi HEA was prepared by vacuum induction melting. The ingot was hot-rolled to 52% thickness at 1000 °C followed by homogenization at 1200 °C for 2 h in an Ar atmosphere and furnace cooling. The homogenized bar was further hot-rolled to 33% thickness at 1000 ˚C. A coarse-grained specimen was prepared by annealing the hot-rolled bar at 800 °C for 1 h in air and subsequent water quenching, hereinafter referred to as CG800. To obtain fine grains, a portion of the homogenized bar was cold-rolled to 94% thickness at ambient temperature. The cold-rolled plates were annealed at 700 or 800 °C for 15 min in air and subsequently water-quenched, hereinafter referred to as FG700 and FG800, respectively. The microstructures were characterized by electron backscatter diffraction (EBSD) and secondary electron imaging with a scanning electron microscope (SEM) (Zeiss, Merlin). The EBSD measurements were conducted at 20 kV with a beam step size of 50 nm after mechanically polishing the specimen surface.

Tensile specimens with gauge dimensions (width × thickness × length) of 2 mm×1 mm×10 mm were obtained by cutting the plates by electric discharge machining. To introduce hydrogen, the tensile specimens were exposed to a 100 MPa hydrogen gas atmosphere at 543 K for 200 h. Tensile tests were carried out at an ambient temperature (20 °C) at initial strain rates of 10^{-4} s^{-1} using a tensile machine (Shimadzu, AGS-10kNX). After the tensile tests, the fracture surface observations were carried out with SEM at 15 kV. Diffusible hydrogen content was measured by thermal desorption spectroscopy (TDS) at a heating rate of 400 °C h^{-1} using a quadrupole mass spectrometer (ESCO, EMD-WA1000S). Diffusible hydrogen content in the present study was defined to be the cumulative hydrogen content from 40 to 600 °C.

3. Results and discussion

In comparison with CG800 results shown in Fig. 1(a), the cold rolling and subsequent

annealing at 800 °C successfully reduced the grain size, as shown in Fig. 1(b). Another difference between CG800 and FG800 was the presence of the σ phase. The formation of the σ phase after annealing has been previously reported in the same HEA [17-19]. The annealing temperatures were the same. However, the annealing time for FG800 was less than that of CG800, which indicates that a stored strain energy, arising from the high dislocation density introduced by cold rolling, enhanced the precipitation. This effect caused the formation of a small amount of the σ phase. The decrease in the annealing temperature, namely for FG700, further decreased the grain size and the grain distribution exhibited a bimodal feature, as shown in Fig. 1(d). A Kernel average misorientation (KAM) in Fig. 1(e), which corresponds to the geometrically necessary dislocation density [20], shows that the values in both the fine and coarse grain regions are low. This indicates that both the fine and coarse grains were fully recrystallized. It is noteworthy that the amount of the σ phase in FG700 was higher than that in FG800, as shown in Fig. 1(f). The average measured grain sizes of CG800, FG800, and FC700 were 22, 1.9, and 1.5 μm, respectively.

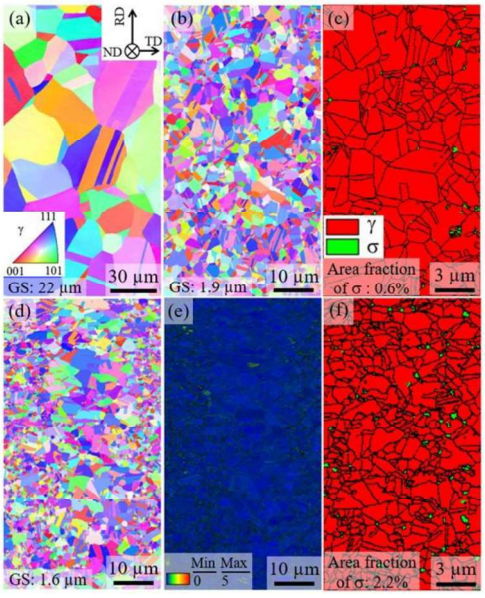

Fig. 1 Sets of EBSD results: (a) RD-IPF map of CG800; (b) RD-IPF and (c) phase maps of FG800; (d) RD-IPF, (e) KAM, and (f) phase maps of FG700. GS: grain size.

Figure 2 shows the hydrogen desorption profiles obtained by the TDS. The diffusible hydrogen contents of CG800, FG800, and FG700, were 113, 129, and 125 mass ppm, respectively. Interestingly, the diffusible hydrogen content did not significantly increase with decreasing grain size (less than 10% variation), while the diffusible hydrogen content in conventional Fe-based alloys, such as austenitic steel [16], ferritic steel [21], and martensitic steel [22], increases with decreasing grain size. Since grain refinement increases the volume fraction of the grain boundary, this fact indirectly indicates that the major site of diffusible hydrogen is not a grain boundary in the HEA, at least before deformation. As the specimens in this study were fully recrystallized, the amounts of vacancy and dislocations in the three specimens do not have significant differences for altering the diffusible hydrogen content. Therefore, the unconventional grain size dependence of diffusible hydrogen content implies that the large amount of the desorbed hydrogen in the HEA was due to hydrogen trapping at interstitial sites of the lattice, which were distorted by the large amount of solute atoms. In addition, an equiatomic quaternary CoCrFeNi alloy, which does not contain Mn, has been reported to show a markedly lower diffusible hydrogen content than that in the CoCrFeMnNi HEA [23]. This indicates that the high diffusible hydrogen content at the interstitial sites in the present experiment is attributed to a Mn-H interaction.

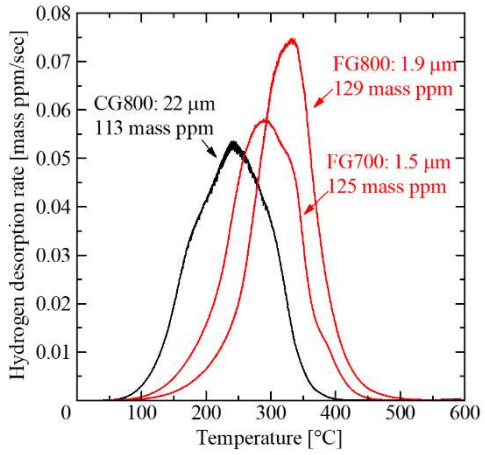

Fig. 2 Hydrogen desorption rate versus temperature at a heating rate of 400 °C h^{-1}.

Figure 3 shows the nominal stress-strain curves. In all of the specimens, the hydrogen uptake caused degradation of the tensile elongation. However, the tensile strength of FG800 did not decrease by the hydrogen uptake, although the strength level was approximately 1.5 times greater than that of CG800. Moreover, the elongation of FG800 with hydrogen was only slightly different from that of CG800 with hydrogen. These results indicate that the grain refinement dramatically improved the strength-elongation balance in the hydrogen-charged condition. The further reduction of the grain size in FG700 increased the strength, but the hydrogen uptake degraded the elongation, strength, and work hardening rate. The significant reduction in the work hardening and associated tensile strength degradation are discussed with the fractographic features below.

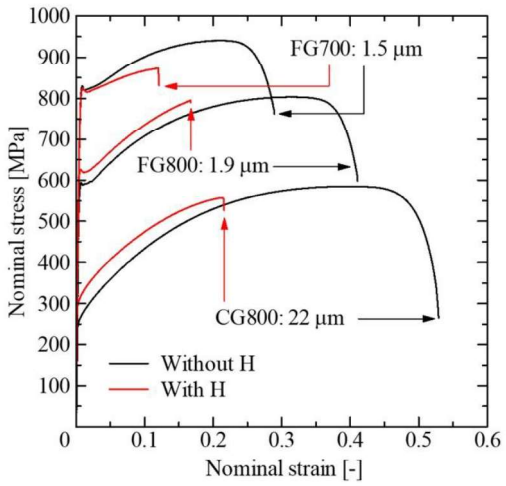

Fig. 3 Nominal stress-strain curves for different grain sizes.

Figure 4 shows images of the fracture surfaces and specimen top surfaces for the grain-refined specimens. As shown in Figs. 4(a) and 4(b), the hydrogen uptake in FG800 changed the fracture mode from ductile to brittle. In particular, an intergranular feature was observed, which was the same as that in CG800 [8]. The intergranular feature has been reported to arise from localized motion and accumulation of dislocations [7,8]. For instance, the localized dislocation accumulation increases local stress near grain boundaries, which assists the grain boundary cracking [7]. In this context, grain refinement moderates stress concentration at grain boundaries [13], which thereby suppresses hydrogen-assisted intergranular fracture even at a high remote stress as observed in FG800 (Fig. 3). Besides, the following three points are noted. (1) The major trap site of the diffusible hydrogen was not the grain boundary as discussed with Fig. 2. (2) The major cracking mode was intergranular, irrespective of grain size. (3) Hydrogen-assisted failures occurred at almost identical strains in CG800 and FG800, as shown in Fig. 3. These facts indicate that hydrogen transport, from grain interior to grain boundaries by dislocation motion, would have a critical role for triggering hydrogen-assisted failure. In addition, spherical patterns were rarely observed as indicated by the yellow arrows in Fig. 4(b) (FG800), which

corresponds to the probability of the σ phase. This indicates that the predominant cracking site in the hydrogen-charged FG800 was along the grain boundaries, and the interface of the σ phase and austenite was a minor cracking site. A change in the fracture mode from ductile to brittle was also observed in FG700, as shown in Figs. 4(c) and 4(d). However, the probability of a spherical pattern for the hydrogen-charged FG700 increased, compared with that of FG800, which is consistent with the increased σ phase fraction. Correspondingly, the specimen top surface of the fractured FG700 without hydrogen exhibited a considerable amount of the σ phase, shown as the white contrast in Fig. 4(e), and that of the fractured FG700 with hydrogen exhibited dimples associated with cracking at the interfaces of σ phase and austenite, as shown in Fig. 4(f). This indicates that one reason for the reductions in the work hardening rate and tensile strength was the frequent cracking at the interface between σ phase and austenite which reduces the cross-sectional area of the specimen.

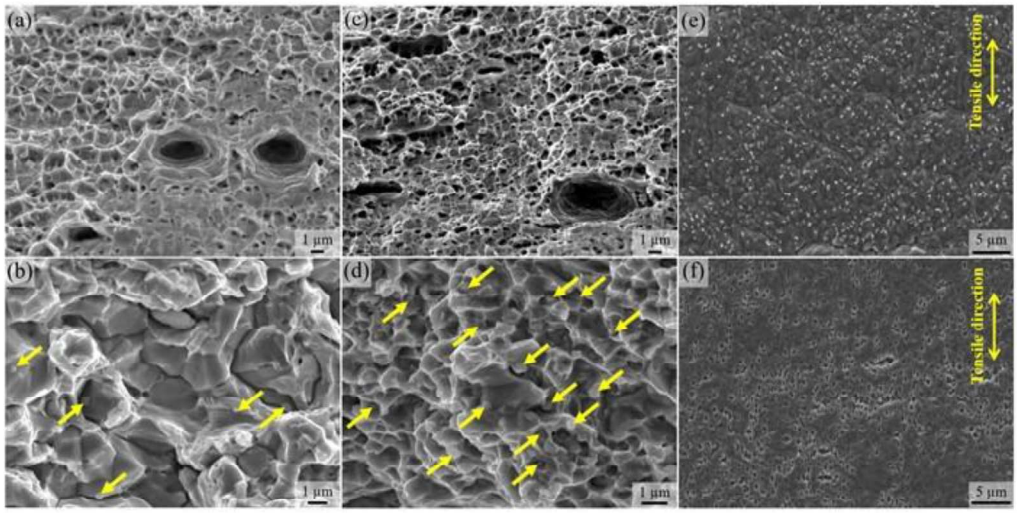

Fig. 4 Fractographs: FG800 (a) without and (b) with hydrogen, and FG700 (c) without and (d) with hydrogen. Specimen surfaces near the fracture surfaces of FG700 (e) without and (f) with hydrogen. The yellow arrows indicate spherical patterns on the fracture surfaces.

4. Conclusions

A significant improvement in hydrogen embrittlement resistance of the equiatomic CoCrFeMnNi HEA by grain refinement was demonstrated. For example, the hydrogen-charged HEA with the grain size of 1.9 μm exhibited a tensile strength that was 1.5 times greater, without a significant decrease in elongation, than that of the hydrogen-charged HEA with the grain size of 22 μm. However, a large amount of the σ phase plays a critical role in the deterioration of the tensile ductility, which occurs when the annealing temperature is low, although low temperature annealing is required to obtain fine grains. Specifically, hydrogen assists cracking at the interfaces of the σ phase and austenite. Therefore, to improve the hydrogen embrittlement resistance through the grain refinement approach, an optimal annealing temperature and time must be selected. An optimal annealing condition determined in this study was 800 °C for 15 min after cold rolling.

Funding: This work was supported by the JSPS KAKENHI [grant numbers JP16H06365, JP17H04956] and the Japan Science and Technology Agency (JST) under the Industry-Academia Collaborative R&D program [grant number 20100113]. MK greatly appreciate Mr. Tatsuo Yokode and Prof. Tatsuya Morikawa for the support of cold rolling.

References

[1] Cantor B. Multicomponent and high entropy alloys. Entropy 2014;16:4749-68.

[2] Yeh JW, Chen SK, Lin SJ, Gan JY, Chin TS, Shun TT, Tsau CH, Chang SY. Nanostructured high-entropy alloys with multiple principal elements: Novel alloy design concepts and outcomes. Adv. Engin. Mater. 2004;6:299–303.

[3] Yao MJ, Pradeep KG, Tasan CC, Raabe D. A novel, single phase, non-equiatomic FeMnNiCoCr high-entropy alloy with exceptional phase stability and tensile ductility. Scr. Mater. 2014;72:5–8.

[4] Gludovatz B, Hohenwarter A, Catoor D, Chang EH, George EP, Ritchie RO. A

fracture-resistant high-entropy alloy for cryonigec applications. Science 2014;345:1153–8.
[5] Luo H, Li Z, Mingers AM, Raabe D. Corrosion behavior of an equiatomic CoCrFeMnNi high-entropy alloy compared with 304 stainless steel in sulfuric acid solution. Corros. Sci. 2018;134:131–9.
[6] Zhao Y, Lee DH, Seok MY, Lee JA, Phaniraj MP, Suh JY, Ha HY, Kim JY, Ramamurty U, Jang JI. Resistance of CoCrFeMnNi high-entropy alloy to gaseous hydrogen embrittlement. Scr. Mater. 2017;135:54–8.
[7] Nygren KE, Bertsch KM, Wang S, Bei H, Nagao A, Robertson IM. Hydrogen embrittlement in compositionally complex FeNiCoCrMn FCC solid solution alloy. Curr. Opin. in Solid State and Mater. Sci. 2018;22:1–7.
[8] Ichii K, Koyama M, Tasan CC, Tsuzaki K. Comparative study of hydrogen embrittlement in stable and metastable high-entropy alloys. Scr. Mater. 2018;150:74–7.
[9] Pu Z, Chen Y, Dai LH. Strong resistance to hydrogen embrittlement of high-entropy alloy. Mater. Sci. Eng. A 2018;736:156–66.
[10] Michler T, Naumann J. Hydrogen environment embrittlement of ausnitic stainless steels at low temperatures. Int. J. Hydrogen Energy 2008;33:2111–22
[11] Michler T, Marchi CS, Naumann J, Weber S. Hydrogen environment embrittlement of stable austenitic steels. Int. J. Hydrogen Energy 2012;37:16231–46.
[12] Koyama M, Akiyama E, Lee YK, Raabe D, Tsuzaki K. Overview of hydrogen embrittlement in high-Mn steels. Int. J. Hydrogen Energy 2017;42:12706–23.
[13] Bai Y, Tian Y, Gao S, Shibata A, Tsuji N. Hydrogen embrittlement behaviors of ultrafine-grained 22Mn-0.6C austenitic twinning induced plasticity steel. J. Mater. Res. 2017;32:4592–604.
[14] Park IJ, Lee SM, Jeon HH, Lee YK. The advantage of grain refinement in the hydrogen embrittlement of Fe-18Mn-0.6C twinning-induced plasticity steel. Corros. Sci. 2015;93:63–9.
[15] Zan N, Ding H, Guo X, Tang Z, Bleck W. Effects of grain size on hydrogen embrittlement in a Fe-22Mn-0.6C TWIP steel. Int. J. Hydrogen Energy 2015;40:10687–96.
[16] Bai Y, Momotani Y, Chen MC, Shibata A, Tsuji N. Effect of grain reginement on hydrogen embrittlement behaviors of high-Mn TWIP steel. Mater. Sci. Eng. A 2016;651:935–44.
[17] Pickering EJ, Muñoz-Moreno R, Stone HJ, Jones NG. Precipitation in the equiatomic high-entropy alloy CrMnFeCoNi. Scr. Mater. 2016;113:106–9.
[18] Stepanov ND, Shaysultanov DG, Ozerov MS, Zherebtsov SV, Salishchev GA. Second phase formation in the CoCrFeNiMn high entropy alloy after recrystallization annealing. Mater. Letters 2016;185:1–4.
[19] Otto F, Dlouhý A, Pradeep KG, Kuběnová M, Raabe D, Eggeler G, George EP. Decomposition of the single-phase high-entropy alloy CrMnFeCoNi after prolonged anneals at

intermediate temperatures. Acta Mater. 2016;112:40–52.
[20] Calcagnotto M, Ponge D, Demir E, Raabe D. Orientation gradients and geometrically necessary dislocations in ultrafine grained dual-phase steels studied by 2D and 3D EBSD. Mater. Sci. Eng. A 2010;527:2738–46.
[21] Park C, Kang N, Liu S. Effect of grain size on the resistance to hydrogen embrittlement of API 2W grade 60 steels using in situ slow-strain-rate testing. Corros. Sci. 2017;128:33–41.
[22] Fuchigami H, Minami H, Nagumo M. Effect of grain size on the susceptibility of martensitic steel to hydrogen-related failure. Philos. Mag. Letters 2006;86:21–9.
[23] Nygren KE, Wang S, Bertsch KM, Bei H, Nagao A, Robertson IM. Hydrogen embrittlement of the equi-molar FeNiCoCr alloy. Acta Mater. 2018;157:218–27.